

:
 : 가 (1. , 2. , 3. , 4.
 : 300, 250, 200, 150 lmg/ml) C-arm , (90 °,
 (45 °), (20 °), (70 °),
 ().
 , , (. .
) 가 . 가
 , , 가 ,
 () .
 : 가 가
 , 가
 300 150 가 200 250 가 .
 : , 가 X
 가 , 가 , X
 가 200 - 250 lmg/ml 가 ,
 가 .
 , ,
 (8 - 10),
 ()
 (1 - 3),
 , 가 가 ,
 (Fig. 1),
 가 .
 (4 - 7).
 ,
 가 ,

1
 2
 3
 4
 5

2003 7 9

2003 10 30

(stainless steel)

가 , DSA (veri - (Feldkamp 's cone beam algorithm/volume rendering)

fication phantom) (10×8×5 cm) (0.998×22 cm) , " high resolution "

(6×6×6 cm) 9 cm 가 가

4 (0.998×9.0 cm) ; /

(0.998×43.5 cm) ; 1 1 (: 1

(, 10 cm; , 4.5 cm) /6).

(2.0×20 cm) C-arm

(2.0×23.5 cm) 57 (, C-arm ; ,

(300 lmg/ml) 90 ° , 70 ° , 45 ° , 20 °

(300, 250, 200, 150 lmg/ml),

(15 cm) (0.4×11 mm)

(1L) ,

(300, 250, 200, 150 lmg/ml)

(bullet rods phantom)

3 (0.2×

3 cm) 3 (4 mm)가 (Fig. 2).

(biplane

DSA unit; Integris Allura biplane, Philips Medical Systems, Best, Netheland) . C-arm 55 °

/sec, 240 ° 120)

(, (Integris 3D RA release 2; Silicon Graphics Inc., Mountain Hill, CA, U.S.A.)

가 30

(4 mm 30 mm) 95%

(one sample T test). 가

(Fig. 3A),

3 (, ,

가 (0, ; 1, ; 2:).

가 ,



Fig. 1. Three-dimensional DSA image of normal internal carotid artery, which is secondarily reconstructed with high resolution.

A. Anterior view of the left internal carotid artery is nicely displayed with good opacity, homogeneity, and sharp margin except for petrous internal carotid artery, anterior and middle cerebral artery (arrows).

B. Superior view shows more blurred margin of the middle cerebral artery than the anterior view (arrowheads).

가 (Fig. 3B, C). 가 가 (Fig. 3D). 가 (Paired (Fig. 3E). Samples Test). (Fig. 3F). (4 mm) (250, 200 Img/ml) 가 (Table 1). (0.029 mm) 95% (0.0225 - 0.0355 mm) (30 mm) (-0.0633 mm) 95% (-0.0742 - - 0.0524 mm) : 가 10% (p value<0.05), 가 (

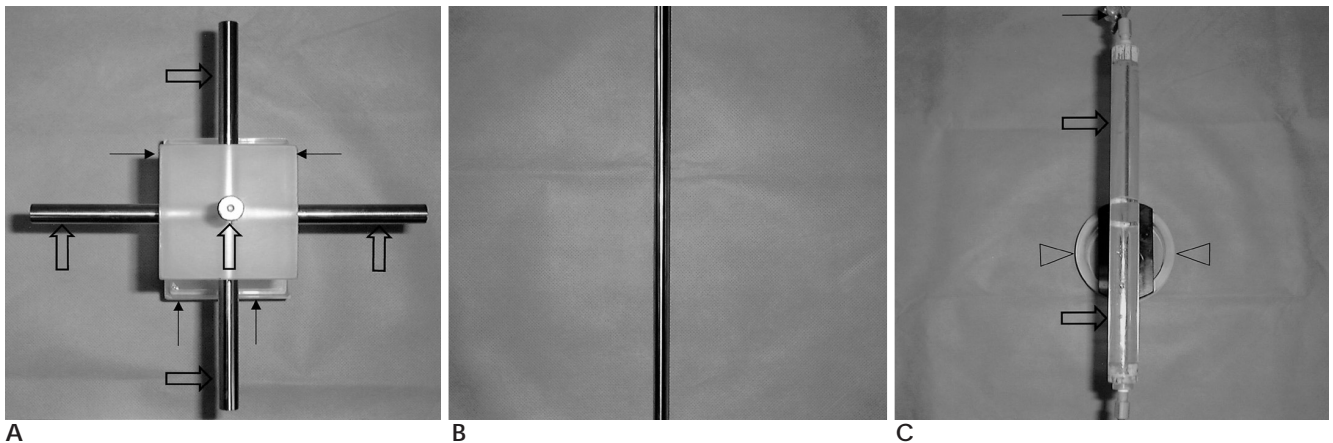


Fig. 2. Five phantoms.

A. The crossed metal rods consist of three crossing right-angled metal rods (open arrows). One acryl cube and another rectangular parallelepiped are overlapped each other (arrows).

B. The one metal rod.

C. The one contrast rod consists of a acryl rod containing contrast (open arrows) with two three ways closing (arrows), a supporting vertically-oriented rod (not shown due to overlapping), and a supporting acryl cylinder (arrow-heads).

D. Fluoroscopic anterior projection of the plastic cup containing one liter of water, and a segment of line of intravenous set containing contrast.

E. Fluoroscopic anterior projection of the verification phantom shows three rods (arrows) and bullets (arrowheads) within an acryl cube.

0.068; , 0.006 mm) 95% (, ,
0.0052 - 0.1308; , - 0.0097 - - 0.0023 mm) (4 - 7).

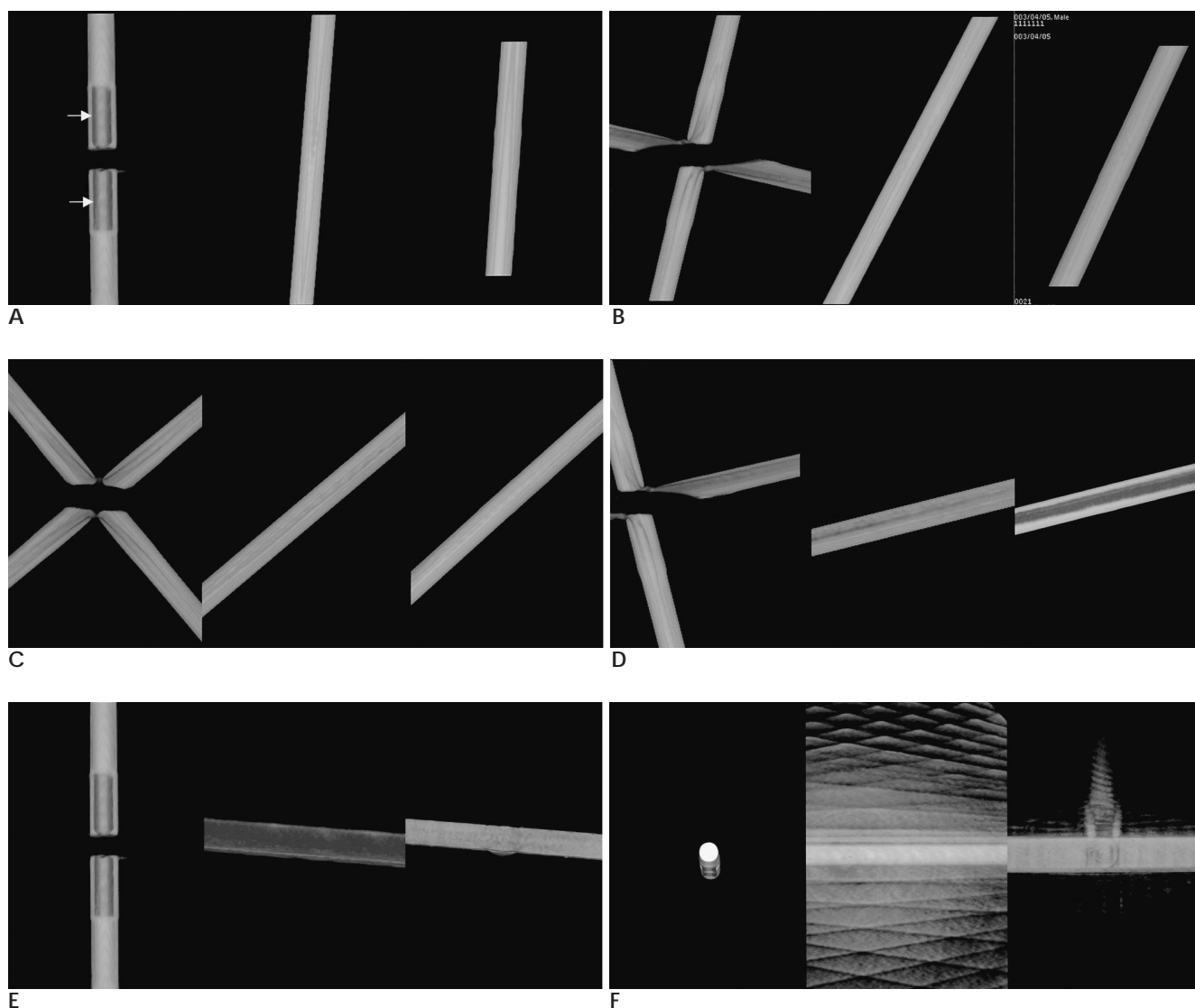


Fig. 3. Three dimensional images of metal and contrast rod phantoms (cross metal rods in the left, one metal rod in the middle, and one contrast rod in the right).

A. Rods of right-angled plane: two rods of rotational plane are not seen on cross metal rod image, which shows an artifact (arrows) resulted from acryl cube in the middle portion of a rod in the right-angled plane.

B. Rods of close to right-angled plane: these phantom images have similar quality to images in **A**.

C. Rods of intermedial plane: these phantom images have similar quality to images in **A**.

D. Rods of close to rotational plane: compared with images in **A**, these three images are graded as intermediate for opacity and margin, which is more evident on superior view (not shown). Only one contrast rod image shows poor homogeneity

E, F. Anterior (**E**) and superior (**F**) view of rods of rotational plane: two rods of this plane of cross metal rods are not seen. One contrast rod image shows intermediate quality in opacity and homogeneity, and poor sharpness of margin on superior view, while cross metal rods and one metal rod images are displayed with lack of or poor opacity, homogeneity, and sharpness of margin. Blurring of margin is much more in one metal rod than in one contrast rod on superior view (**F**).

Table 1. Grading of the Three-dimensional Image Quality of Phantoms

	Opacity	Homogeneity	Margin sharpness
Cross metal rods			
Rotational	poor	poor	poor
Close to rotational	intermediate	intermediate	intermediate
One metal rod			
Rotational	poor	poor	poor
Close to rotational	intermediate	intermediate	intermediate
One contrast rod			
Rotational	intermediate	intermediate	poor
Close to rotational	intermediate	poor	intermediate
Contrast (300 Img/ml) in water			
Rotational	intermediate	poor	poor
Close to rotational	intermediate	intermediate	intermediate
Contrast (250 Img/ml) in water			
Rotational	intermediate	intermediate	intermediate
Close to rotational	intermediate	intermediate	good
Contrast (200 Img/ml) in water			
Rotational	intermediate	intermediate	intermediate
Close to rotational	intermediate	intermediate	good
Contrast (150 Img/ml) in water			
Rotational	poor	poor	poor
Close to rotational	intermediate	intermediate	good

Grades for intermedial, close to right-angle, and right-angle planes are high in all three items of all phantoms.

(11). 0.0524 mm) 가 가 .

(44 - 120), (Algebraic or Cone beam 가 가 .

algorithm), (Pincushion , S , 가 가 .

) (volume rendering, surface 가 가 . Bridcut (11)

rendering, maximum intensity projection), volume - rendered 3D DSA (100)

(20 - 208 mm 가 - 1.1

(- 1.4 mm (- 1.0 - 2.3%) . 20 mm

가

(4 -

7) 가 (44) 1 cm

가 , 1 cm

(20) DSA , 4 mm 30 mm

가 가

가

가 C-arm 90 °

가 가

(Tanigawa (12)

4.5 mm, 10, 20, 30, 40, 50 mm

(, 0.73%; , 0.21%) 95% (44 /) DSA

(, 0.0225 - 0.0355 mm; , - 0.0742 - - 30 mm

1. Heautot JF, Chabert E, Gandon Y, et al. Analysis of cerebrovascular diseases by a new 3-dimensional computerized X-ray angiography system. *Neuroradiology* 1998;40:203-209
2. Saint-Felix D, Troussset Y, Picard C, Ponchut C, Romeas R, Rougee A. In vivo evaluation of a new system for 3-D computerized angiography. *Phy Med Biol* 1994;39:583-595
3. Tu RK, Cohen WA, Maravilla KR, et al. Digital subtraction rotational angiography for aneurysms of the intracranial anterior circulation: injection method and optimization. *AJNR Am J Neuroradiol* 1996;17:1127-1136
4. Hochmuth A, Spetzger U, Schumacher M. Comparison of three-dimensional rotational angiography with digital subtraction angiography in the assessment of ruptured cerebral aneurysms. *AJNR Am J Neuroradiol* 2002;23:1199-1205
5. Kiyosue H, Tanoue S, Okahara M, et al. Anatomic features predictive of complete aneurysm occlusion can be determined with three-dimensional digital subtraction angiography. *AJNR Am J Neuroradiol* 2002;23:1206-1213
6. Anxionnat R, Bracard S, Ducrocq X, et al. Intracranial aneurysms: clinical value of 3D digital subtraction angiography in the therapeutic decision and endovascular treatment. *Radiology* 2001;218:799-808
7. Sugahara T, Korogi Y, Nakashima K, Hamatake S, Honda S, Takahashi M. Comparison of 2D and 3D digital subtraction angiography in evaluation of intracranial aneurysms. *AJNR Am J Neuroradiol* 2002;23:1545-1552
8. Connors JJ 3rd, Wojak JC. Percutaneous transluminal angioplasty for intracranial atherosclerotic lesions: evolution of technique and short-term results. *J Neurosurg* 1999;91:415-423
9. Levy EI, Horowitz MB, Koebe CJ, et al. Transluminal stent-assisted angioplasty of the intracranial vertebrobasilar system for medically refractory, posterior circulation ischemia: early results. *Neurosurgery* 2001;48:1215-1223
10. Lee JH, Kwon SU, Lee JH, Suh DC, Kim JS. Percutaneous transluminal angioplasty for symptomatic middle cerebral artery stenosis: long-term follow-up. *Cerebrovasc Dis* 2003;15:90-97
11. Bridcut RR, Winder RJ, Workman A, Flynn P. Assessment of distortion in a three-dimensional rotational angiography system. *Br J Radiol* 2002;75:266-270
12. Tanigawa H, Sakaguchi T, Abe T, Hyodo K, Hokimoto K, Hayabuchi N. Experimental study of pseudo-stenosis artifact on three-dimensional DSA. *Nippon Hoshasen Gijutsu Gakkai Zasshi* 2002;58:1687-1695

A Phantom Study for Revealing Factors Related to Image Distortion of Three-Dimensional Reconstruction Rotational Angiogram¹

Bae Ju Kwon, M.D., Moon Hee Han, M.D.^{1,2,3}, Seung-Rho Lee, M.D.⁴,
Chang Kok Hahm, M.D.⁴, Hee-Chan Kim, Ph.D.⁵, Kee-Hyun Chang, M.D.^{1,2,3}

¹Department of Radiology, Seoul National University College of Medicine

²Clinical Research Institute, Seoul National University Hospital

³Institute of Radiation Medicine, Seoul National University Medical Research Center

⁴Department of Radiology, Hanyang University College of Medicine

⁵Biomedical engineering, Seoul National University College of Medicine

Purpose: To determine, by means of a phantom study, the distortion-related factors and appropriate iodine concentration for three-dimensional reconstruction rotational angiography.

Materials and Methods: Four phantoms were created: crossed metal rods, one metal rod, one contrast rod, and a contrast rod under water. Iodine concentrations were 300, 250, 200, and 150 Img/ml, respectively. For each phantom, rotational angiography was performed in the rotational, right-angled (90 ° to rotational), intermedial (45 °), close to rotational (20 °), and close to right-angled (70 °) planes. Two-dimensional projection images were transferred to a workstation at which 3D images were produced using the volume rendering technique. Image quality in each plane was evaluated in terms of opacity, homogeneity, and margin sharpness, which were graded as low, intermediate or high by two neuroradiologists who used images obtained in the right-angled plane as the standard reference. The same assessors evaluated in terms of the same parameters, cross-sectional images obtained at the central, intermedial, and peripheral portions of one metal rod positioned in the right-angled, close to right-angled, and intermedial planes, and in order to compare the values at different sites, one neuroradiologist measured the horizontal and vertical diameters of each cut image.

Results: Three-dimensional images of all four phantoms were high quality in the close to right-angled and intermedial plane, but in the rotational and close to rotational plane were degraded. In particular, metal rod images obtained in the rotational plane were poor for all three items. In these two planes, image quality was better for the contrast rod than the metal rod, and at 200 and 250 Img/ml concentrations than at 300 and 150 Img/ml concentrations. There was no significant difference in image quality, nor in measured values of the diameter between cut images.

Conclusion: A three-dimensional image was more distorted when a linear object was placed at a lesser angle to the rotational plane and when inherent X-ray attenuation was greater, a finding which must be closely related to the beam-hardening artifact. Distortion was least at 200 - 250 Img/ml of iodine concentration, the concentration thought to be most appropriate for *in-vitro* 3D angiography.

Index words : Digital subtraction angiography
Images, artifact
Cerebral blood vessels

Address reprint requests to : Moon Hee Han, M.D. Ph.D., Department of Diagnostic Radiology, Seoul National University Hospital,
28 Yongsong-dong, Chongno-gu, Seoul 110-744, Korea.
Tel. 82-2-760-3602 Fax. 82-2-743-6385 E-mail: hanmh@radcom.snu.ac.kr